ARTICLE IN PRESS

Journal of Computational Physics xxx (2009) xxx–xxx

Contents lists available at ScienceDirect

Journal of Computational Physics

journal homepage: www.elsevier.com/locate/jcp

A splitting method for incompressible flows with variable density based on a pressure Poisson equation

J.-L. Guermond *,[1], Abner Salgado

Department of Mathematics, Texas A&M University, 3368 TAMU, College Station, TX 77843 3368, USA

ARTICLE INFO

Article history:
Received 21 May 2008
Received in revised form 10 December 2008
Accepted 18 December 2008
Available online xxxx

MSC:
65N30
76M05

Keywords:
Variable density flows
Navier–Stokes
Projection method
Fractional time-stepping

ABSTRACT

A new fractional time-stepping technique for solving incompressible flows with variable density is proposed. The main feature of this method is that, as opposed to other known algorithms, the pressure is determined by just solving one Poisson equation per time step, which greatly reduces the computational cost. The stability of the method is proved and the performance of the method is numerically illustrated.

1. Introduction

This paper deals with the numerical approximation of incompressible viscous flows with variable density. This type of flows are governed by the time-dependent Navier–Stokes equations:

$$\begin{cases} \rho_t + \nabla\cdot(\rho\mathbf{u}) = 0, \\ \rho(\mathbf{u}_t + \mathbf{u}\cdot\nabla\mathbf{u}) + \nabla p - \mu\Delta\mathbf{u} = \mathbf{f}, \\ \nabla\cdot\mathbf{u} = 0, \end{cases} \tag{1.1}$$

where the dependent variables are the density $\rho > 0$, the velocity field $\mathbf{u}$, and the pressure p. The constant μ is the dynamic viscosity coefficient and $\mathbf{f}$ is a driving external force. In stratified flows we typically have $\mathbf{f} = \rho\mathbf{g}$, where $\mathbf{g}$ is the gravity field. The fluid occupies a bounded domain Ω in $\mathbb{R}^d$ (with $d = 2$ or 3) and a solution to the above problem is sought over a time interval $[0,T]$. The Navier–Stokes system is supplemented by the following initial and boundary conditions for $\mathbf{u}$ and ρ:

$$\begin{cases} \rho(\mathbf{x},0) = \rho_0(\mathbf{x}), \quad \rho(\mathbf{x},t)|_{\Gamma^-} = a(\mathbf{x},t), \\ \mathbf{u}(\mathbf{x},0) = \mathbf{u}_0(\mathbf{x}), \quad \mathbf{u}(\mathbf{x},t)|_{\Gamma} = \mathbf{b}(\mathbf{x},t), \end{cases} \tag{1.2}$$

* Corresponding author.
E-mail addresses: guermond@limsi.fr, guermond@math.tamu.edu (J.-L. Guermond).
[1] On long leave from LIMSI (CNRS-UPR 3251), BP 133, 91403, Orsay, France.

0021-9991/$ - see front matter © 2008 Elsevier Inc. All rights reserved.
doi:10.1016/j.jcp.2008.12.036

where $\Gamma = \partial\Omega$ and Γ^- is the inflow boundary, which is defined by $\Gamma^- = \{\mathbf{x} \in \Gamma : \mathbf{u}(\mathbf{x}) \cdot \mathbf{n} < 0\}$, with $\mathbf{n}$ being the outward unit normal vector. Throughout this paper we assume that the boundary Γ is impermeable, i.e., $\mathbf{u} \cdot \mathbf{n} = 0$ everywhere on Γ, and $\Gamma^- = \emptyset$.

The mathematical theory of existence and uniqueness for (1.1) and (1.2) is quite involved and we refer to Lions [22] for further details. The difficulty comes from the fact that these equations entangle hyperbolic, parabolic, and elliptic features. Approximating (1.1) and (1.2) efficiently is a challenging task. A testimony of the difficulty is that, so far, very few papers have been dedicated to the mathematical analysis of the approximation of (1.1) and (1.2). We refer to Liu and Walkington [23] for one of the few attempts in this direction.

Approximating (1.1) and (1.2) can be done by solving the coupled system (1.1), but this approach is computer intensive due to the elliptic character induced by incompressibility. Alternative, more efficient, approaches advocated in the literature consist of using fractional time-stepping and exploiting, as far as possible, techniques already established for the solution of constant density incompressible fluid flows. The starting point of most fractional time-stepping algorithms consists of decoupling the incompressibility constraint and diffusion in the spirit of Chorin's [5] and Temam's [28] projection method. Several algorithms have been developed which extend this idea to the situation that concerns us here, see for example [2,1,18,24]. To the best of our knowledge, Guermond and Quartapelle [18] gave the first stability proof of a projection method for variable density flows. The algorithm proposed in [18] is somewhat expensive since it is composed of two time-consuming projections. An alternative algorithm composed of only one projection per time step was proposed in [24] and proved to be stable. It seems that so far [18,24] are the only papers where projection methods for variable density flows have been proved to be stable, the best available results being that of Pyo and Shen [24].

The common feature of all the projection-like methods referred to above is that at each time step, say t^{n+1}, the pressure or some related scalar quantity, say Φ, is determined by solving an equation of the following form:

$$-\nabla \cdot \left(\frac{1}{\rho^{n+1}} \nabla \Phi\right) = \Psi, \quad \partial_n \Phi|_\Gamma = 0, \tag{1.3}$$

where ρ^{n+1} is an approximation of the density at time t^{n+1} and Ψ is some right-hand side that varies at each time step. The problem (1.3) is far more complicated to solve than just a Poisson equation. It is time consuming since it requires assembling and pre-conditioning a variable-coefficient stiffness matrix at each time step. Note also that, it is necessary to have a uniform lower bound on the value of the density for (1.3) to be solvable. This condition is a key to the method that we propose and it seems that it has not been given enough attention in the literature.

The objective of the present work is to introduce a fractional time-stepping method for solving variable density flows that involves solving only one Poisson problem per time step instead of problems like (1.3). The proposed algorithm is proved to be stable and numerically illustrated.

The paper is organized as follows: in Section 2 we introduce the non-incremental version of our method and prove its stability. The incremental version of the method is introduced in Section 3. First-order Euler time stepping is used in Sections 2 and 3. The most accurate version of the method using second-order Backward Second Difference (BDF2) is presented in Section 4. Finally, Section 5 contains some numerical experiments that demonstrate the performance of the method.

2. Non-incremental projection method

To introduce the main characteristics of the method, we first focus our attention on its simplest form, which, using the terminology from Guermond et al. [13], we henceforth refer to as the non-incremental version. More elaborate versions of this method are introduced in the subsequent sections.

2.1. The heuristic argument

Let us start by reviewing the usual non-incremental Chorin/Temam algorithm for constant density [5,28,25,26]. We partition the time interval $[0,T]$ into N subintervals, which for the sake of simplicity we take uniform. We then introduce the time step $\Delta t = T/N$ and the discrete times $t_n = n\Delta t$, for $n \in \{0,\dots,N\}$. For the time being, let us neglect the nonlinear terms to simplify the argumentation. Then the non-incremental Chorin/Temam algorithm for solving the constant density time-dependent Stokes equations consists of computing two sequences of approximate velocities $\{\tilde{\mathbf{u}}^{n+1}\}_{n=0,\dots,N}$, $\{\mathbf{u}^{n+1}\}_{n=0,\dots,N}$, and one sequence of approximate pressure $\{p^{n+1}\}_{n=0,\dots,N}$ as follows: First, set $\mathbf{u}^0 = \mathbf{u}_0$, then for all time steps t^{n+1}, $n \geqslant 0$, solve

$$\frac{\rho}{\Delta t}(\tilde{\mathbf{u}}^{n+1} - \mathbf{u}^n) - \mu \Delta \tilde{\mathbf{u}}^{n+1} = \mathbf{f}^{n+1}, \quad \tilde{\mathbf{u}}^{n+1}|_\Gamma = 0, \tag{2.1}$$

and

$$\frac{1}{\Delta t}(\mathbf{u}^{n+1} - \tilde{\mathbf{u}}^{n+1}) + \frac{1}{\rho} \nabla p^{n+1} = 0, \quad \nabla \cdot \mathbf{u}^{n+1} = 0, \quad \mathbf{u}^{n+1} \cdot \mathbf{n}|_\Gamma = 0, \tag{2.2}$$

where we have set $\mathbf{f}^{n+1} := \mathbf{f}(t^{n+1})$. One key observation is that the second sub-step can be interpreted as a projection. Indeed, this sub-step can be recast as follows:

Please cite this article in press as: J.-L. Guermond, A. Salgado, A splitting method for incompressible flows with variable density ..., J. Comput. Phys. (2009), doi:10.1016/j.jcp.2008.12.036

$$\mathbf{u}^{n+1}+\frac{\Delta t}{\rho}\nabla p^{n+1}=\tilde{\mathbf{u}}^{n+1},\quad \nabla\cdot\mathbf{u}^{n+1}=0,\quad \mathbf{u}^{n+1}\cdot\mathbf{n}|_{\Gamma}=0, \tag{2.3}$$

which is the Helmholtz decomposition of $\tilde{\mathbf{u}}^{n+1}$ into a solenoidal part with zero normal trace plus a gradient. Upon introducing the Hilbert space

$$\mathbf{H}=\{\mathbf{v}\in\mathbf{L}^2(\Omega):\nabla\cdot\mathbf{v}=0;\ \mathbf{v}\cdot\mathbf{n}|_{\Gamma}=0\}, \tag{2.4}$$

the above decomposition can be equivalently rewritten $\mathbf{u}^{n+1}=P_{\mathbf{H}}\tilde{\mathbf{u}}^{n+1}$, where $P_{\mathbf{H}}$ is the $\mathbf{L}^2$-projection onto $\mathbf{H}$. This fact is the reason this method together with its many avatars is often referred to as a projection algorithm. One very interesting feature of (2.1) and (2.2) is that the pressure is computed by solving the following Poisson problem:

$$\Delta p^{n+1}=\frac{\rho}{\Delta t}\nabla\cdot\tilde{\mathbf{u}}^{n+1},\quad \partial_n p^{n+1}|_{\Gamma}=0. \tag{2.5}$$

The algorithm (2.1) and (2.2) is simple and can be proved to converge. Higher-order generalizations can be constructed and there exist convergence proofs up to second-order in time for the $\mathbf{L}^2$-norm of the velocity for some of these algorithms, see e.g. [30,27,11,4,19]. A comprehensive review on these methods is done in Guermond et al. [13].

It is important to note at this point that to infer (2.5) from (2.2) we used the fact that the density is constant. When the density is not constant, most of the attempts at splitting the pressure and the velocity that we are aware of so far are based on strategies that are similar to that described above. The main idea always consists of projecting a non-solenoidal provisional velocity onto $\mathbf{H}$; in other words, most of the currently known splitting algorithms consist of solving problems similar to (2.2). When taking the divergence of the left-most equation in (2.2) one is then reduced to solve a problem like the following:

$$-\nabla\cdot\left(\frac{1}{\rho^{n+1}}\nabla\Phi\right)=\Psi,\quad \partial_n\Phi|_{\Gamma}=0, \tag{2.6}$$

where ρ^{n+1} is an approximation of the non constant function $\rho(t^{n+1})$. It seems that all the algorithms that are more or less based on the Helmholtz decomposition (2.3) always lead to problems like (2.6), which are hard to solve efficiently due to the $1/\rho^{n+1}$ variable coefficient. The key conceptual leap proposed in the present paper consists of abandoning the projection point of view in favor of a penalty-like argument.

As emphasized in Guermond [10] and Guermond and Quartapelle [16], the projected velocity $\mathbf{u}^{n+1}$ can be eliminated from (2.1) and (2.2). More precisely, the two sub-steps in (2.1) and (2.2) can be equivalently recast as follows:

$$\frac{\rho}{\Delta t}(\tilde{\mathbf{u}}^{n+1}-\tilde{\mathbf{u}}^{n})-\mu\Delta\tilde{\mathbf{u}}^{n+1}+\nabla p^{n}=\mathbf{f}^{n+1},\quad \tilde{\mathbf{u}}^{n+1}|_{\Gamma}=0, \tag{2.7}$$

and

$$\Delta p^{n+1}=\frac{\rho}{\Delta t}\nabla\cdot\tilde{\mathbf{u}}^{n+1},\quad \partial_n p^{n+1}|_{\Gamma}=0. \tag{2.8}$$

Once $\mathbf{u}^{n+1}$ is eliminated, it is clear that the Chorin/Temam algorithm is a discrete version of the following perturbation of the Navier–Stokes equations:

$$\begin{cases}\rho(\mathbf{u}_t+\mathbf{u}\cdot\nabla\mathbf{u})+\nabla p-\mu\Delta\mathbf{u}=\mathbf{f}, & \mathbf{u}|_{\Gamma}=0,\\ \nabla\cdot\mathbf{u}-\frac{\epsilon}{\rho}\Delta p=0, & \partial_n p|_{\Gamma}=0,\end{cases} \tag{2.9}$$

where $\epsilon:=\Delta t$. Actually, this perturbation is nothing more than a penalty on the divergence of the velocity as recognized in Rannacher [25], since the momentum equation can also be recast into

$$\rho(\mathbf{u}_t+\mathbf{u}\cdot\nabla\mathbf{u})+\rho\epsilon^{-1}\nabla\Delta^{-1}\nabla\cdot\mathbf{u}-\mu\Delta\mathbf{u}=\mathbf{f}, \tag{2.10}$$

where Δ^{-1} is the inverse of the Laplace operator equipped with homogeneous Neumann boundary conditions. That is, given $\Psi\in L^2(\Omega)$, we denote by $\Phi=\Delta^{-1}\Psi\in H^1(\Omega)$ the function that has zero mean value and solves

$$\langle\nabla\Phi,\nabla r\rangle=\langle\Psi,r\rangle,\quad \forall r\in H^1(\Omega), \tag{2.11}$$

where $\langle\cdot,\cdot\rangle$ denotes the scalar product in $L^2(\Omega)$. No notational distinction is made between scalar products in $L^2(\Omega)$ and $\mathbf{L}^2(\Omega)$.

The major claim of the present paper is that adopting the penalty point of view stated in (2.9) yields efficient splitting algorithms whether the density is constant or not. This point of view is somewhat orthogonal to the current mainstream in the literature which mainly focuses on the projection point of view.

Remark 2.1. Note that (2.10) is significantly different from standard penalty techniques using $-\epsilon^{-1}\nabla\nabla\cdot\mathbf{u}$ as penalty term, which are generally ill-conditioned. These techniques penalize the divergence in L^2 whereas the term $\epsilon^{-1}\nabla\Delta^{-1}\nabla\cdot\mathbf{u}$ penalize it in a weak norm somewhat related to that of $H^{-1}:=(H_0^1)'$.

Please cite this article in press as: J.-L. Guermond, A. Salgado, A splitting method for incompressible flows with variable density ..., J. Comput. Phys. (2009), doi:10.1016/j.jcp.2008.12.036

2.2. The non-incremental scheme

For the reader who is familiar with penalty techniques, it is clear that provided ϵ is small enough the divergence of the velocity field solving (2.10) is small and $\rho\epsilon^{-1}\Delta^{-1}\nabla\cdot\mathbf{u}$ is an approximation of the pressure. We are now going to construct an algorithm based on these two observations.

First we construct a penalty coefficient that is dimensionally correct. For this purpose we define

$$\rho_0^{\min} := \min_{\mathbf{x}\in\Omega}\rho_0(\mathbf{x}).$$

Henceforth we assume that $\rho_0^{\min}>0$, i.e., there is no vacuum. Second, we choose a number χ in the interval $(0,\rho_0^{\min}]$, i.e.,

$$\chi\in(0,\rho_0^{\min}]. \tag{2.12}$$

In the computations reported at the end of the paper we take $\chi=\rho_0^{\min}$. By setting $\epsilon := \Delta t/\chi$, we have defined a penalty coefficient with the correct dimension.

We now define the approximate sequences $\{\rho^n\}_{n=0,\dots,N}$, $\{\mathbf{u}^n\}_{n=0,\dots,N}$, and $\{p^n\}_{n=0,\dots,N}$ as follows: Set $\rho^0=\rho_0$, $\mathbf{u}^0=\mathbf{u}_0$, $p^0=0$, and for all time index n ranging 0 to $N-1$ solve:

$$\frac{\rho^{n+1}-\rho^n}{\Delta t}+\nabla\cdot(\rho^{n+1}\mathbf{u}^n)-\frac{\rho^{n+1}}{2}\nabla\cdot\mathbf{u}^n=0, \tag{2.13}$$

$$\rho^n\frac{\mathbf{u}^{n+1}-\mathbf{u}^n}{\Delta t}+\rho^{n+1}(\mathbf{u}^n\cdot\nabla)\mathbf{u}^{n+1}-\mu\Delta\mathbf{u}^{n+1}+\frac{\rho^{n+1}}{4}(\nabla\cdot\mathbf{u}^n)\mathbf{u}^{n+1}+\nabla p^n=\mathbf{f}^{n+1},\quad \mathbf{u}^{n+1}|_\Gamma=0, \tag{2.14}$$

$$\Delta p^{n+1}=\frac{\chi}{\Delta t}\nabla\cdot\mathbf{u}^{n+1},\quad \partial_n p^{n+1}|_\Gamma=0, \tag{2.15}$$

The density equation (2.13) is obtained using a first-order semi-implicit discretization of the mass conservation equation in (1.1). The additional term $\frac{\rho^{n+1}}{2}\nabla\cdot\mathbf{u}^n$ is consistent since it is zero if $\nabla\cdot\mathbf{u}^n=0$, and its meaning will become clear when we do the stability analysis.

The velocity equation (2.14) is obtained by approximating the momentum equation in (1.1) using a first-order semi-implicit discretization similar to that for the density. The additional term is also consistent and it is added to obtain unconditional stability. When the density is constant, the above algorithm (without the transport term) is the same as (2.7) and (2.8) where, to simplify the notation, we have dropped the tilde from $\tilde{\mathbf{u}}^n$ and $\tilde{\mathbf{u}}^{n+1}$, since this is the only velocity family that we will be using from now on.

The pressure equation (2.15) is a penalty equation in the spirit of (2.9).

Remark 2.2. Note that (2.15) is a standard Poisson equation, i.e., the above algorithm does not contain any second-order PDE with non-constant coefficients like (2.6). This is the main novelty of the present paper.

2.3. Stability analysis of the non-incremental scheme

To avoid irrelevant technicalities, we assume that there is no external driving force, i.e., $\mathbf{f}=0$. We henceforth denote by $\|\cdot\|$ the L^2-norm. No notational distinction is made between the norm in $L^2(\Omega)$ and $\mathbf{L}^2(\Omega)$.

We start with the L^2-stability of the density.

Proposition 2.1. *For any $\Delta t>0$ and any sequence of velocities $\{\mathbf{u}^n\}_{n=0,\dots,N}$ in $\mathbf{L}^\infty(\Omega)$ with bounded divergence and satisfying $\mathbf{u}^n\cdot\mathbf{n}|_\Gamma=0$, the solution to (2.13) satisfies:*

$$\|\rho^N\|^2+\sum_{k=0}^{N-1}\|\rho^{k+1}-\rho^k\|^2=\|\rho_0\|^2.$$

Proof. Let us multiply (2.13) by $2\Delta t\rho^{n+1}$ and integrate over Ω. Using the identity $2a\cdot(a-b)=a^2-b^2+(a-b)^2$ we obtain

$$\|\rho^{n+1}\|^2-\|\rho^n\|^2+\|\rho^{n+1}-\rho^n\|^2+2\Delta t\int_\Omega\nabla\cdot\big(\rho^{n+1}\mathbf{u}^n\big)\rho^{n+1}-\Delta t\int_\Omega(\rho^{n+1})^2\nabla\cdot\mathbf{u}^n=0.$$

Taking into account the boundary condition on $\mathbf{u}^n$ and integrating by parts, we infer

$$\begin{aligned}2\int_\Omega\nabla\cdot(\rho^{n+1}\mathbf{u}^n)\rho^{n+1}-\int_\Omega(\rho^{n+1})^2\nabla\cdot\mathbf{u}^n&=-2\int_\Omega\rho^{n+1}\mathbf{u}^n\cdot\nabla\rho^{n+1}-\int_\Omega(\rho^{n+1})^2\nabla\cdot\mathbf{u}^n\\&=-\int_\Omega\mathbf{u}^n\cdot\nabla[(\rho^{n+1})^2]-\int_\Omega(\rho^{n+1})^2\nabla\cdot\mathbf{u}^n=-\int_\Omega\nabla\cdot[(\rho^{n+1})^2u^n]=0.\end{aligned}$$

Adding up the equality

$$\|\rho^{n+1}\|^2-\|\rho^n\|^2+\|\rho^{n+1}-\rho^n\|^2=0,$$

from $n=0$ to $n=N-1$, we obtain the desired result. □

Please cite this article in press as: J.-L. Guermond, A. Salgado, A splitting method for incompressible flows with variable density ..., J. Comput. Phys. (2009), doi:10.1016/j.jcp.2008.12.036

Remark 2.3. Note that the above stability result for the density does not depend on the incompressibility constraint, i.e., the field $\mathbf{u}^n$ does not need to be solenoidal. This is important, since the approximate velocity solving (2.14) is not solenoidal. The unconditional stability is due to the extra term $\frac{\rho^{n+1}}{2}\nabla\cdot\mathbf{u}^n$. The origin of this term can be traced back to Temam [29].

Having established the stability of (2.13), we prove stability of the algorithm (2.14) and (2.15) under the assumption of the existence of a uniform lower bound on the density. More precisely we make the following technical assumption: The sequence $\{\rho^n\}_{n=0,\ldots,N}$ satisfies the following:

$$\{\rho^n\}_{n=0,\ldots,N} \text{ is uniformly bounded in } L^\infty(\Omega), \tag{2.16}$$

$$\forall n=0,\ldots,N,\quad \chi\leqslant\rho^n(x),\ \text{a.e. in } \Omega. \tag{2.17}$$

Theorem 2.1. *Assume that (2.16) and (2.17) hold. Then, for any $\Delta t>0$ the solution to (2.14) and (2.15) satisfies the following inequality:*

$$\sum_{k=1}^{N}\|\sigma^k\mathbf{u}^k\|^2+2\mu\Delta t\sum_{k=1}^{N}\|\nabla\mathbf{u}^k\|^2+\frac{(\Delta t)^2}{\chi}\left[\sum_{k=1}^{N}\|\nabla p^k\|^2+\sum_{k=0}^{N-1}\|\nabla p^k\|^2\right]\leqslant\|\sigma_0\mathbf{u}_0\|^2,$$

where $\sigma^n:=\sqrt{\rho^n}$.

Proof. We first multiply the momentum equation (2.14) by $2\Delta t\mathbf{u}^{n+1}$, integrate by parts, and use the identity $2a\cdot(a-b)=a^2-b^2+(a-b)^2$. We obtain

$$\begin{aligned}&\|\sigma^n\mathbf{u}^{n+1}\|^2-\|\sigma^n\mathbf{u}^n\|^2+\|\sigma^n(\mathbf{u}^{n+1}-\mathbf{u}^n)\|^2+2\mu\Delta t\|\nabla\mathbf{u}^{n+1}\|^2+\Delta t\int_\Omega\rho^{n+1}\mathbf{u}^n\cdot\nabla|\mathbf{u}^{n+1}|^2\\&\quad+\frac{\Delta t}{2}\int_\Omega\rho^{n+1}(\nabla\cdot\mathbf{u}^n)|\mathbf{u}^{n+1}|^2+2\Delta t\langle\nabla p^n,\mathbf{u}^{n+1}\rangle=0.\end{aligned}\tag{2.18}$$

Next, we multiply the density equation (2.13) by $\Delta t|\mathbf{u}^{n+1}|^2$ and integrate by parts. We obtain

$$\|\sigma^{n+1}\mathbf{u}^{n+1}\|^2-\|\sigma^n\mathbf{u}^{n+1}\|^2-\Delta t\int_\Omega\rho^{n+1}\mathbf{u}^n\cdot\nabla|\mathbf{u}^{n+1}|^2-\frac{\Delta t}{2}\int_\Omega\rho^{n+1}(\nabla\cdot\mathbf{u}^n)|\mathbf{u}^{n+1}|^2=0.\tag{2.19}$$

Adding up Eqs. (2.18) and (2.19) we obtain

$$\|\sigma^{n+1}\mathbf{u}^{n+1}\|^2-\|\sigma^n\mathbf{u}^n\|^2+\|\sigma^n(\mathbf{u}^{n+1}-\mathbf{u}^n)\|^2+2\mu\Delta t\|\nabla\mathbf{u}^{n+1}\|^2+2\Delta t\langle\nabla p^n,\mathbf{u}^{n+1}\rangle=0.\tag{2.20}$$

Taking Eq. (2.15) at time steps $n+1$ and n and subtracting one from the other, and using Cauchy–Schwarz inequality and Hypothesis (2.17), we infer that

$$(\Delta t)^2\|\nabla(p^{n+1}-p^n)\|^2\leqslant\chi^2\|\mathbf{u}^{n+1}-\mathbf{u}^n\|^2\leqslant\|\sigma^n(\mathbf{u}^{n+1}-\mathbf{u}^n)\|^2.\tag{2.21}$$

Multiplying (2.15) by $2(\Delta t)^2p^n$ and integrating over Ω we derive

$$2\Delta t\langle\mathbf{u}^{n+1},\nabla p^n\rangle=2\chi^{-1}(\Delta t)^2\langle\nabla p^{n+1},\nabla p^n\rangle=\chi^{-1}(\Delta t)^2[\|\nabla p^{n+1}\|^2+\|\nabla p^n\|^2-\|\nabla(p^{n+1}-p^n)\|^2],\tag{2.22}$$

Adding (2.20) and (2.21), and using (2.22) we obtain

$$\|\sigma^{n+1}\mathbf{u}^{n+1}\|^2-\|\sigma^n\mathbf{u}^n\|^2+2\mu\Delta t\|\nabla\mathbf{u}^{n+1}\|^2+\chi^{-1}(\Delta t)^2[\|\nabla p^{n+1}\|^2+\|\nabla p^n\|^2]\leqslant0.$$

which when we add up over $n=0,\ldots,N-1$ gives the desired stability result. □

Remark 2.4. Hypothesis (2.17) is rarely explicitly mentioned in numerical papers based on algorithms using (1.3), see e.g. [1,2,18,24], but it is required to guarantee well-posedness. It seems that this condition is often overlooked. We do not want to discuss in details how (2.17) can be achieved and proved, since this issue is non-trivial and goes far beyond the scope of the present paper. Suffices to say that this can be achieved for instance by using so-called monotone schemes. We refer for instance to Walkington [32] for a scheme using a discontinuous Galerkin technique. The numerical examples presented at the end of this paper have been computed using a shock-capturing technique for which we observed that (2.17) is always satisfied. The details of this shock-capturing technique are reported in [14,15].

Remark 2.5. Theorem 2.1 is a conditional result since we have not established that (2.13) guarantees (2.17), i.e., $\chi\leqslant\rho^n$ for all $n=0,\ldots,N$. We introduce in the next section an algorithm that decouples even further the mass conservation and the momentum conservation so that the impact of the discretization of the mass conservation is minimized and reduced to ascertaining (2.17).

Remark 2.6. The quantity $\frac{1}{2}\|\sigma^n\mathbf{u}^n\|^2$ is the kinetic energy of the flow. Hence it is more natural to establish bounds in terms of this quantity than on the velocity itself; see also Lions [22].

Please cite this article in press as: J.-L. Guermond, A. Salgado, A splitting method for incompressible flows with variable density ..., J. Comput. Phys. (2009), doi:10.1016/j.jcp.2008.12.036

3. Incremental projection method

It is now well established that the non-incremental pressure correction method is low-order accurate. More precisely, the error is $\mathcal{O}(\Delta t)$ for the velocity in the $\mathbf{L}^2$-norm and $\mathcal{O}\left(\Delta t^{\frac{1}{2}}\right)$ for the velocity in the $\mathbf{H}^1$-norm and the pressure in the L^2-norm; see e.g. [25,26,17]. We now introduce an incremental version of the method to overcome this accuracy deficiency. We use the same notation as in the previous section and, under the same assumptions on the density, we prove that this method is stable.

3.1. The heuristic argument

Chorin/Temam's constant density algorithm can be improved by making the pressure explicit in the viscous step and by correcting it in the projection step. This technique is usually referred to as the incremental pressure-correction algorithm. This algorithm consists of computing two sequences of approximate velocities $\{\tilde{\mathbf{u}}^{n+1}\}_{n=0,\cdots,N}$, $\{\mathbf{u}^{n+1}\}_{n=0,\cdots,N}$, and one sequence of approximate pressure $\{p^{n+1}\}_{n=0,\cdots,N}$ as follows: First, set $\mathbf{u}^0=\mathbf{u}_0$, $p^0=p(0)$, compute an approximation of $\mathbf{u}^1:=\mathbf{u}(\Delta t)$, then for all time steps t^{n+1}, $n>0$, solve

$$\frac{\rho}{\Delta t}(\tilde{\mathbf{u}}^{n+1}-\mathbf{u}^n)-\mu\Delta\tilde{\mathbf{u}}^{n+1}+\nabla p^n=\mathbf{f}^{n+1},\quad \tilde{\mathbf{u}}^{n+1}|_\Gamma=0, \tag{3.1}$$

and

$$\frac{1}{\Delta t}(\mathbf{u}^{n+1}-\tilde{\mathbf{u}}^{n+1})+\frac{1}{\rho}\nabla\phi^{n+1}=0,\quad \nabla\cdot\mathbf{u}^{n+1}=0,\quad \mathbf{u}^{n+1}\cdot\mathbf{n}|_\Gamma=0, \tag{3.2}$$

$$p^{n+1}=p^n+\phi^{n+1}. \tag{3.3}$$

We refer the reader to Shen [26] and Guermond and Quartapelle [16] for the analysis of the scheme (3.1), (3.2) and (3.3). By proceeding as in Section 2.1, the so-called projected velocity (i.e., the solenoidal one) can be algebraically eliminated and once this is done and difference quotients are replaced by time derivatives and the remaining Δt's are replaced by ϵ, the above algorithm reduces to the following perturbation of the Navier–Stokes equations:

$$\begin{cases}\rho(\mathbf{u}_t+\mathbf{u}\cdot\nabla\mathbf{u})+\nabla p-\mu\Delta\mathbf{u}=\mathbf{f}, & \mathbf{u}|_\Gamma=0,\\ \nabla\cdot\mathbf{u}-\frac{\epsilon}{\rho}\Delta\phi=0, & \partial_n\phi|_\Gamma=0,\\ \epsilon p_t=\phi.\end{cases} \tag{3.4}$$

Formally (3.4) is a $\mathcal{O}(\epsilon^2)$ perturbation of the constant density incompressible Navier–Stokes equations. By proceeding again as in Section 2.1 we are now going to use (3.4) as the starting point for a new algorithm for variable density flows.

First set $\rho^0=\rho_0$, $\mathbf{u}^0=\mathbf{u}_0$, and $\phi^0=0$. Let p_0 be the pressure at $t=0$ and set $p^0=p_0$. This quantity can be deduced from ρ^0 and $\mathbf{u}_0$. For instance if the flow is at rest at $t=0$, then $p_0=0$. We define χ as in (2.12). Then, given $\{(\rho^n,\mathbf{u}^n,p^n,\phi^n)\}_{n=0,\cdots,N-1}$ we advance in time in the following way: The density is updated using the same relation as before

$$\frac{\rho^{n+1}-\rho^n}{\Delta t}+\nabla\cdot(\rho^{n+1}\mathbf{u}^n)-\frac{\rho^{n+1}}{2}\nabla\cdot\mathbf{u}^n=0. \tag{3.5}$$

The velocity is now updated using

$$\frac{1}{\Delta t}\left[\frac{1}{2}(\rho^{n+1}+\rho^n)\mathbf{u}^{n+1}-\rho^n\mathbf{u}^n\right]+\rho^{n+1}\mathbf{u}^n\cdot\nabla\mathbf{u}^{n+1}+\frac{1}{2}\nabla\cdot(\rho^{n+1}\mathbf{u}^n)\mathbf{u}^{n+1}-\mu\Delta\mathbf{u}^{n+1}+\nabla(p^n+\phi^n)=\mathbf{f}^{n+1},\quad \mathbf{u}^{n+1}|_\Gamma=0. \tag{3.6}$$

The variable ϕ is updated using

$$\Delta\phi^{n+1}=\frac{\chi}{\Delta t}\nabla\cdot\mathbf{u}^{n+1},\quad \partial_n\phi^{n+1}|_\Gamma=0, \tag{3.7}$$

and, finally, the pressure is updated by

$$p^{n+1}=p^n+\phi^{n+1}. \tag{3.8}$$

Remark 3.1. The pressure term in the momentum equation (3.6) is a second-order extrapolation of the pressure at time t^{n+1}, since using (3.8) at time step n we have

$$p^n+\phi^n=2p^n-p^{n-1}.$$

Please cite this article in press as: J.-L. Guermond, A. Salgado, A splitting method for incompressible flows with variable density ..., J. Comput. Phys. (2009), doi:10.1016/j.jcp.2008.12.036

Remark 3.2. The term $\frac{1}{\Delta t}\left[\frac{1}{2}(\rho^{n+1}+\rho^n)\mathbf{u}^{n+1}-\rho^n\mathbf{u}^n\right]+\frac{1}{2}\nabla\cdot(\rho^{n+1}\mathbf{u}^n)\mathbf{u}^{n+1}$ is asymptotically consistent with the equation. Notice that if the involved functions are sufficiently smooth

$$\begin{aligned}\frac{\frac{1}{2}(\rho^{n+1}+\rho^n)\mathbf{u}^{n+1}-\rho^n\mathbf{u}^n}{\Delta t}+\frac{1}{2}\nabla\cdot(\rho^{n+1}\mathbf{u}^n)\mathbf{u}^{n+1}&=\frac{(\rho^{n+1}-\rho^n)}{2\Delta t}\mathbf{u}^{n+1}+\rho^n\frac{(\mathbf{u}^{n+1}-\mathbf{u}^n)}{\Delta t}+\frac{1}{2}\nabla\cdot(\rho^{n+1}\mathbf{u}^n)\mathbf{u}^{n+1}\\&=\frac{1}{2}(\rho_t+\nabla\cdot(\rho\mathbf{u}))^{n+1}\mathbf{u}^{n+1}+(\rho\mathbf{u}_t)^{n+1}+\mathcal{O}(\Delta t)=(\rho\mathbf{u}_t)^{n+1}+\mathcal{O}(\Delta t),\end{aligned}$$

The purpose of this particular way of discretizing the quantity $\rho\mathbf{u}_t$ is to further decouple the mass conservation and the momentum conservation equations. This will become clear once we do the stability analysis.

Remark 3.3. By analogy with projection methods for constant density flows [30,19], we can write a rotational version of the above algorithm by replacing the pressure update (3.8) by

$$p^{n+1}=p^n+\phi^{n+1}-\mu\nabla\cdot\mathbf{u}^{n+1}. \tag{3.9}$$

3.2. Stability analysis of the incremental scheme

We assume again that $\mathbf{f}=0$ to avoid irrelevant technicalities. Note that the equation used to determine the density is the same as in the non-incremental case. Therefore, the L^2-stability of the density is again a consequence of Proposition 2.1.

Theorem 3.1. *Assume that (2.16) and (2.17) hold. Then, for any $\Delta t>0$ the solution to (3.6)–(3.8) satisfies*

$$\|\sigma^N\mathbf{u}^N\|^2+2\mu\Delta t\sum_{k=1}^{N}\|\nabla\mathbf{u}^k\|^2+\frac{(\Delta t)^2}{\chi}\|\nabla p^N\|^2+\frac{(\Delta t)^2}{\chi}\sum_{k=1}^{N-1}\|\nabla(p^k-p^{k-1})\|^2\leqslant\|\sigma_0\mathbf{u}_0\|^2+\frac{(\Delta t)^2}{\chi}\|\nabla p_0\|^2,$$

where $\sigma^n=\sqrt{\rho^n}$.

Proof. We take the momentum equation (3.6), multiply it by $2\Delta t\mathbf{u}^{n+1}$ and integrate. Notice that the boundary conditions imply

$$\begin{aligned}\int_\Omega\left[\rho^{n+1}\mathbf{u}^n\cdot\nabla\mathbf{u}^{n+1}+\frac{1}{2}\nabla\cdot(\rho^{n+1}\mathbf{u}^n)\mathbf{u}^{n+1}\right]\cdot\mathbf{u}^{n+1}&=\int_\Omega\left[\rho^{n+1}\mathbf{u}^n\cdot\nabla\frac{|\mathbf{u}^{n+1}|^2}{2}+\nabla\cdot(\rho^{n+1}\mathbf{u}^n)\frac{|\mathbf{u}^{n+1}|^2}{2}\right]\\&=\int_\Omega\nabla\cdot\left[\rho^{n+1}\frac{|\mathbf{u}^{n+1}|^2}{2}\mathbf{u}^n\right]=0.\end{aligned}$$

Next, we have

$$\begin{aligned}\left\langle\frac{\frac{1}{2}(\rho^{n+1}+\rho^n)\mathbf{u}^{n+1}-\rho^n\mathbf{u}^n}{\Delta t},2\Delta t\mathbf{u}^{n+1}\right\rangle&=\|\sigma^{n+1}\mathbf{u}^{n+1}\|^2+\langle\rho^n(\mathbf{u}^{n+1}-2\mathbf{u}^n),\mathbf{u}^{n+1}\rangle\\&=\|\sigma^{n+1}\mathbf{u}^{n+1}\|^2+\|\sigma^n(\mathbf{u}^{n+1}-\mathbf{u}^n)\|^2-\|\sigma^n\mathbf{u}^n\|^2.\end{aligned}$$

By combining the above observations, we arrive at the following equality

$$\|\sigma^{n+1}\mathbf{u}^{n+1}\|^2-\|\sigma^n\mathbf{u}^n\|^2+\|\sigma^n(\mathbf{u}^{n+1}-\mathbf{u}^n)\|^2+2\mu\Delta t\|\nabla\mathbf{u}^{n+1}\|^2+2\Delta t\langle\nabla(p^n+\phi^n),\mathbf{u}^{n+1}\rangle=0. \tag{3.10}$$

By (3.8), we infer

$$-2\Delta t\langle\nabla(p^n+\phi^n),\mathbf{u}^{n+1}\rangle=-2\Delta t\langle\nabla(2p^n-p^{n-1}),\mathbf{u}^{n+1}\rangle=2\Delta t\langle\nabla(p^{n+1}-2p^n+p^{n-1}),\mathbf{u}^{n+1}\rangle-2\Delta t\langle\nabla p^{n+1},\mathbf{u}^{n+1}\rangle. \tag{3.11}$$

Now, we rewrite (3.7) as follows:

$$\Delta(p^{n+1}-p^n)-\frac{\chi}{\Delta t}\nabla\cdot\mathbf{u}^{n+1}=0,$$

then we multiply this identity by $2(\Delta t)^2(p^{n+1}-2p^n+p^{n-1})/\chi$, and, after integrating by parts, we obtain

$$-2\frac{(\Delta t)^2}{\chi}\langle\nabla(p^{n+1}-p^n),\nabla(p^{n+1}-p^n)-\nabla(p^n-p^{n-1})\rangle+2\Delta t\langle\mathbf{u}^{n+1},\nabla(p^{n+1}-2p^n-p^{n-1})\rangle=0.$$

Using again the identity $2a\cdot(a-b)=a^2-b^2+(a-b)^2$ we obtain

$$\frac{(\Delta t)^2}{\chi}\left[-\|\nabla(p^{n+1}-p^n)\|^2+\|\nabla(p^n-p^{n-1})\|^2-\|\nabla(p^{n+1}-2p^n+p^{n-1})\|^2\right]+2\Delta t\langle\mathbf{u}^{n+1},\nabla(p^{n+1}-2p^n-p^{n-1})\rangle=0. \tag{3.12}$$

Please cite this article in press as: J.-L. Guermond, A. Salgado, A splitting method for incompressible flows with variable density ..., J. Comput. Phys. (2009), doi:10.1016/j.jcp.2008.12.036

Multiplying Eq. (3.7) by $2(\Delta t)^2 p^{n+1}/\chi$, we get

$$\frac{(\Delta t)^2}{\chi}[\|\nabla p^{n+1}\|^2 - \|\nabla p^n\|^2 + \|\nabla(p^{n+1}-p^n)\|^2] = 2\Delta t\langle \mathbf{u}^{n+1}, \nabla p^{n+1}\rangle, \tag{3.13}$$

where we integrated by parts and used the identity mentioned before.

Finally, taking (3.7) at time step $n+1$ and subtracting (3.7) at time step n, and using the lower bound Hypothesis (2.17), we derive the following estimate

$$\frac{(\Delta t)^2}{\chi}\|\nabla(p^{n+1}-2p^n+p^{n-1})\|^2 \leqslant \chi\|\mathbf{u}^{n+1}-\mathbf{u}^n\|^2 \leqslant \|\sigma^n(\mathbf{u}^{n+1}-\mathbf{u}^n)\|^2. \tag{3.14}$$

Adding (3.10)–(3.14), we obtain

$$\|\sigma^{n+1}\mathbf{u}^{n+1}\|^2 - \|\sigma^n\mathbf{u}^n\|^2 + 2\mu\Delta t\|\nabla\mathbf{u}^{n+1}\|^2 + \frac{(\Delta t)^2}{\chi}[\|\nabla p^{n+1}\|^2 - \|\nabla p^n\|^2 + \|\nabla(p^n-p^{n-1})\|^2] \leqslant 0.$$

The desired result is obtained by adding up these relations for $n = 0,\ldots,N-1$. □

Remark 3.4. Although numerical tests (see below) reveal that the rotational version of algorithm (3.6), (3.7) and (3.9) is stable and convergent, we have not yet been able to prove stability.

3.3. Space discretization

We now describe a conforming space discretization for the above time splitting algorithm. We assume that we have at hand families of finite-dimensional vector spaces to approximate the velocity, the pressure, and the density fields, respectively,

$$\mathbf{X}_h \subset \mathbf{H}_0^1(\Omega), \quad M_h \subset H^1_{f=0}(\Omega), \quad W_h \subset H^1(\Omega). \tag{3.15}$$

The velocity space $\mathbf{X}_h$ and pressure space M_h are assumed to be compatible, in the sense that they satisfy the so-called LBB condition [3,9,7].

It is well known that the Galerkin method is not well suited for solving hyperbolic equations (see for instance [7]). The list of techniques aiming at addressing this problem is endless; in this list one can cite Galerkin-Least-Squares [20], Discontinuous-Galerkin [21,32], subgrid viscosity [12], method of characteristics [6] and many others. We will assume that the numerical solution of (3.5) is obtained by one of these stabilization techniques and that the sequence $\{\rho_h^n\}_{n=0,\ldots,N} \subset W_h$, satisfies the hypotheses (2.16) and (2.17).

We set $\rho_h^0 = \rho_{0h}$, $\mathbf{u}_h^0 = \mathbf{u}_{0h}$, $p_h^0 = p_{0h}$ and $\phi_h^0 = 0$ where $\rho_{0h} \in W_h$, $\mathbf{u}_{0h} \in \mathbf{X}_h$ and $p_{0h} \in M_h$ are suitable approximations of ρ_0, $\mathbf{u}_0$ and p_0, respectively. Then, the fully discretized algorithm proceeds as follows: Given $(\rho_h^n, \mathbf{u}_h^n, p_h^n, \phi_h^n) \in W_h \times \mathbf{X}_h \times M_h \times M_h$

$$\text{compute } \rho_h^{n+1} \text{ so that (2.16) and (2.17) hold.} \tag{3.16}$$

Solve for $\mathbf{u}_h^{n+1} \in \mathbf{X}_h$ so that

$$\begin{aligned}&\frac{1}{\Delta t}\langle\frac{1}{2}(\rho_h^{n+1}+\rho_h^n)\mathbf{u}_h^{n+1}, \mathbf{v}_h\rangle + \mu\langle\nabla\mathbf{u}_h^{n+1}, \nabla\mathbf{v}_h\rangle + \langle\rho_h^{n+1}\mathbf{u}_h^n\cdot\nabla\mathbf{u}_h^{n+1}, \mathbf{v}_h\rangle + \frac{1}{2}\langle\nabla\cdot(\rho_h^{n+1}\mathbf{u}_h^n)\mathbf{u}_h^{n+1}, \mathbf{v}_h\rangle\\ &\quad = -\langle\nabla(p_h^n+\phi_h^n), \mathbf{v}_h\rangle + \langle\mathbf{f}^{n+1}, \mathbf{v}_h\rangle + \frac{1}{\Delta t}\langle\rho_h^n\mathbf{u}_h^n, \mathbf{v}_h\rangle, \quad \forall\mathbf{v}_h \in \mathbf{X}_h.\end{aligned} \tag{3.17}$$

Solve for $\phi_h^{n+1} \in M_h$, so that

$$\langle\nabla\phi_h^{n+1}, \nabla q_h\rangle = \frac{\chi}{\Delta t}\langle\mathbf{u}_h^{n+1}, \nabla q_h\rangle, \quad \forall q_h \in M_h. \tag{3.18}$$

Finally, update the new pressure $p_h^{n+1} \in M_h$ by setting

$$p_h^{n+1} = p_h^n + \phi_h^{n+1}. \tag{3.19}$$

The above algorithm is stable in the following sense:

Corollary 3.1. *Assume that the sequence $\{\rho_h^n\}_{n=0,\ldots,N} \subset W_h$, satisfies the hypotheses (2.16) and (2.17). Then, for any $\Delta t > 0$ the solution to (3.17)–(3.19) satisfies*

$$\|\sigma_h^N\mathbf{u}_h^N\|^2 + 2\mu\Delta t\sum_{k=1}^{N}\|\nabla\mathbf{u}_h^k\|^2 + \frac{(\Delta t)^2}{\chi}\|\nabla p_h^N\|^2 + \frac{(\Delta t)^2}{\chi}\sum_{k=1}^{N-1}\|\nabla(p_h^k-p_h^{k-1})\|^2 \leqslant \|\sigma_{0h}\mathbf{u}_{0h}\|^2 + \frac{(\Delta t)^2}{\chi}\|\nabla p_{0h}\|^2, \tag{3.20}$$

where $\sigma_h^n = \sqrt{\rho_h^n}$.

Please cite this article in press as: J.-L. Guermond, A. Salgado, A splitting method for incompressible flows with variable density ..., J. Comput. Phys. (2009), doi:10.1016/j.jcp.2008.12.036

Proof. The proof is essentially the same as that of Theorem 3.1. To realize this, it is sufficient to notice that all the test functions that we use are admissible in the corresponding discrete spaces. □

Remark 3.5. The above algorithm is an improvement over the second-order algorithm described in Pyo and Shen [24, Algorithm 2], which requires a very strong (somewhat unrealistic) compatibility condition between the density and velocity spaces.

Remark 3.6. As usual for fractional time stepping techniques for the Stokes and Navier–Stokes equations, the stability property from Corollary 3.1 does not explicitly require the pair of spaces $(\mathbf{X}_h, M_h)$ to satisfy the LBB condition. This impression is misleading, since (3.20) does not really give a realistic stability on the pressure (unless $\Delta t \geqslant c\, h$). When going through the details one eventually realizes that the LBB condition must be invoked to prove stability on the pressure in $L^2(\Omega)$, we refer the reader to, e.g. [10,11,13] for more details on this issue.

4. BDF second-order rotational projection method

The method presented in the previous section has a second-order splitting error (see [11, Theorem 5.1] for the constant density version of this argument). But, to obtain a scheme of formal second-order accuracy in time it is necessary to replace the two-level semi-implicit time discretization used in the mass conservation and momentum equations with a second-order accurate time stepping method. The purpose of this section is to rewrite the rotational version of the incremental pressure-correction algorithm described above by using the three-level BDF2 method.S

We proceed as before. The starting point is the BDF2 version of the rotational pressure-correction algorithm for constant density flows, see e.g. [19]. The main idea consists of eliminating the so-called projected velocity and rewriting the projection step in the form of a Poisson equation where the constant density is replaced by χ; we refer to formulae 3.17, 3.18 and 3.19 from [13] with $p^{\star,k+1} = p^k, \beta_2 = \frac{3}{2}, \beta_1 = -\frac{1}{2}$, and $\beta_0 = 2$. The above program is realized as follows: first initialize $(\rho^0, \mathbf{u}^0, p^0, \phi^0)$ and $(\rho^1, \mathbf{u}^1, p^1, \phi^1)$. For instance $(\rho^1, \mathbf{u}^1, p^1, \phi^1)$ can be computed by using one step of the first-order algorithm described in the previous Section. Then for $n \geqslant 1$, introduce the linearly extrapolated velocity field at the new time level $n+1$ by defining

$$\mathbf{u}^\star = 2\mathbf{u}^n - \mathbf{u}^{n-1}.$$

The new density ρ^{n+1} is evaluated by solving the following discretized version of the mass conservation equation:

$$\frac{3\rho^{n+1} - 4\rho^n + \rho^{n-1}}{2\Delta t} + \mathbf{u}^\star \cdot \nabla \rho^{n+1} = 0. \tag{4.1}$$

Similarly, the momentum equation is discretized in time as follows:

$$\rho^{n+1}\frac{3\mathbf{u}^{n+1} - 4\mathbf{u}^n + \mathbf{u}^{n-1}}{2\Delta t} + \rho^{n+1}(\mathbf{u}^\star \cdot \nabla)\mathbf{u}^{n+1} - \mu\Delta\mathbf{u}^{n+1} + \nabla\left(p^n + \frac{4}{3}\phi^n - \frac{\phi^{n-1}}{3}\right) = \mathbf{f}^{n+1}, \quad \mathbf{u}^{n+1}|_\Gamma = 0. \tag{4.2}$$

A pressure correction is evaluated by solving

$$\Delta\phi^{n+1} = \frac{3\chi}{2\Delta t}\nabla \cdot \mathbf{u}^{n+1}, \quad \partial_n \phi^{n+1}|_\Gamma = 0. \tag{4.3}$$

Finally, the pressure is updated by means of

$$p^{n+1} = p^n + \phi^{n+1} - \mu\nabla \cdot \mathbf{u}^{n+1}. \tag{4.4}$$

The key difference between the above algorithm and 3.17, 3.18 and 3.19 from [13] is that the density is now variable and there is the χ coefficient in (4.3).

Note that we did not add any particular extra stabilization terms in (4.1) and (4.2), the main reason being that the stability analysis of the method still eludes us at the moment; nevertheless, numerical experiments (see Section 5) show that this method is indeed stable and accurate.

5. Numerical experiments

5.1. Convergence tests

In order to test the algorithm (4.1)–(4.3) and (4.4), we consider a problem with a known analytical solution. We solve the variable density Navier–Stokes equations in the unit disk

$$\Omega = \{(x, y) \in \mathbb{R}^2 : x^2 + y^2 < 1\},$$

Please cite this article in press as: J.-L. Guermond, A. Salgado, A splitting method for incompressible flows with variable density ..., J. Comput. Phys. (2009), doi:10.1016/j.jcp.2008.12.036

having the exact solution

$$\rho(x,y,t) = 2 + x\cos(\sin(t)) + y\sin(\sin(t)),$$
$$\mathbf{u}(x,y,t) = \begin{pmatrix} -y\cos(t) \\ x\cos(t) \end{pmatrix},$$
$$p(x,y,t) = \sin(x)\sin(y)\sin(t),$$

so that the right-hand side to the momentum equation is

$$\mathbf{f} = \begin{pmatrix} \rho(x,y,t)(y\sin(t) - x\cos^2(t)) + \cos(x)\sin(y)\sin(t) \\ -\rho(x,y,t)(x\sin(t) + y\cos^2(t)) + \sin(x)\cos(y)\sin(t) \end{pmatrix}.$$

Using the second-order scheme of Section 4 and a $(\mathbb{P}_2, \mathbb{P}_2, \mathbb{P}_1)$ discretization for the density–velocity–pressure, we solve the above mentioned problem for $T = 10$. The mesh size is chosen small enough so that the error from the discretization in space is negligible compared to the time stepping error. The time steps tested are in the range $3.125 \times 10^{-3} \leqslant \Delta t \leqslant 10^{-1}$ The results are shown in Table 1. We have measured the maximum in time of the error of all variables in the indicated spaces. As we see, the time discretization error is second-order for all the quantities. There is a slight degradation of the convergence rate on the density due to the fact that we use the Galerkin method with no extra stabilization. In the tests reported in the next section the Galerkin method is stabilized using a shock-capturing technique based on the residual equation for the square of the density.

Remark 5.1. Note that for constant density flows it has been proved [19] (see also [13]) that the error in time in the L^2-norm for the pressure and in the $\mathbf{H}^1$-norm for the velocity is not fully second-order but rather of order $\frac{3}{2}$ in domains with piecewise smooth boundary. In the results that we obtained all the quantities have second-order accuracy in time and we conjecture that this is due to the regularity of the domain (Ω is a disk). In general domains (i.e., with piecewise smooth boundary) we expect second-order for the velocity in the $\mathbf{L}^2$-norm and $\frac{3}{2}$-order for the pressure the L^2-norm and the velocity in the $\mathbf{H}^1$-norm.

5.2. A low Atwood number problem

We now illustrate the performance of the method on a realistic problem. We compute the development of a Rayleigh–Taylor instability in the viscous regime as documented by Tryggvason in [31]. This problem consists of two layers of fluid initially at rest in the rectangular domain $\Omega = (-d/2, d/2) \times (-2d, 2d)$. The transition between the two fluids is regularized as follows:

$$\frac{\rho(x,y,t=0)}{\rho_0^{\min}} = 2 + \tanh\left(\frac{y - \eta(x)}{0.01d}\right), \tag{5.1}$$

where the initial position of the perturbed interface is $\eta(x) = -0.1d\cos(2\pi x/d)$. The heavy fluid is above and the density ratio is 3, so that the Atwood number

$$A_t = (\rho_0^{\max} - \rho_0^{\min})/(\rho_0^{\max} + \rho_0^{\min}), \tag{5.2}$$

equals 0.5, according to Tryggvason's definition, where we set $\rho_0^{\max} := \max_{\mathbf{x}\in\Omega}\rho_0(\mathbf{x})$. For $t > 0$ the system evolves under the action of a vertical downward gravity field of intensity $\mathbf{g}$; the source term in the momentum equation is downward and equal to ρg.

The equations are non-dimensionalized using the following references: $\rho_0^{\min}$ for the density, d for lengths, and $d^{1/2}/g^{1/2}$ for time, where g is the gravity field. Then, the reference velocity is $d^{1/2}g^{1/2}$, and the Reynolds number is defined by $Re = \rho_0^{\min} d^{3/2} g^{1/2}/\mu$. The computational domain can be restricted to $(0, d/2) \times (-2d, 2d)$ since we assume that the symmetry of the initial condition is maintained during the time evolution. The no-slip condition is enforced at the bottom and top walls and symmetry is imposed on the two vertical sides.

The mass conservation equation is stabilized by adding a nonlinear viscosity proportional to the residual of the conservation equation for ρ^2 in the spirit of the entropy viscosity of [14]. This technique is very efficient and details will be reported elsewhere [15].

Table 1
Error in time for second-order scheme.

Δt	Velocity L^2	Rate	Velocity H^1	Rate	Pressure L^2	Rate	Density L^2	Rate
0.100000	3.90E−3	–	1.63E−2	–	1.25E−2	–	1.25E−2	–
0.050000	1.18E−3	1.73	5.03E−3	1.70	3.61E−3	1.79	2.93E−3	2.09
0.025000	3.35E−4	1.82	1.47E−3	1.77	1.00E−3	1.85	7.60E−4	1.95
0.012500	9.04E−5	1.89	4.13E−4	1.83	2.70E−4	1.89	2.08E−4	1.87
0.006250	2.37E−5	1.93	1.15E−4	1.84	7.10E−5	1.93	5.85E−5	1.83
0.003125	6.12E−6	1.95	3.17E−5	1.86	1.87E−5	1.93	1.67E−5	1.81

Please cite this article in press as: J.-L. Guermond, A. Salgado, A splitting method for incompressible flows with variable density ..., J. Comput. Phys. (2009), doi:10.1016/j.jcp.2008.12.036

The time evolution of the density field at $Re = 1000$ is shown in Fig. 1 at times 1, 1.5, 1.75, 2, 2.25, and 2.5 in the time scale of Tryggvason, which is related to ours by $t_{\text{Tryg}} = t\sqrt{A_t}$. The mesh is composed of 232,552 triangles and there are 466,573 $\mathbb{P}_2$ nodes. The mesh size is of order *0.025* in the refined regions. The time step is $\Delta t = 0.00125\sqrt{A_t}$.

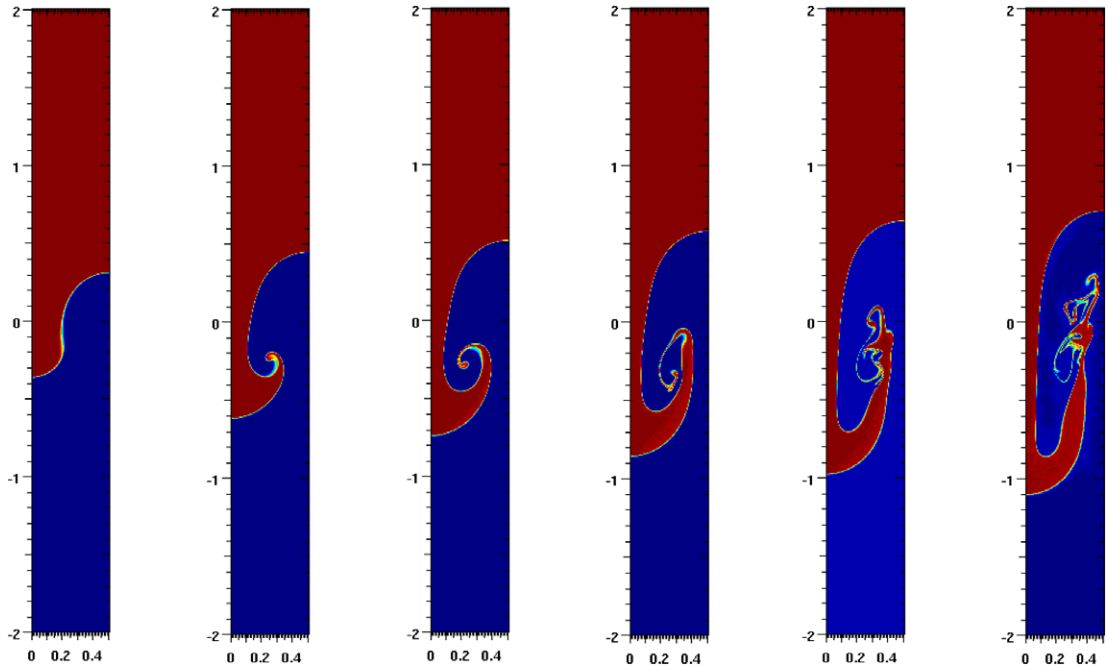

Fig. 1. $Re = 1000$; density ratio 3. The interface is shown at times 1, 1.5, 1.75, 2, 2.25, and 2.5.

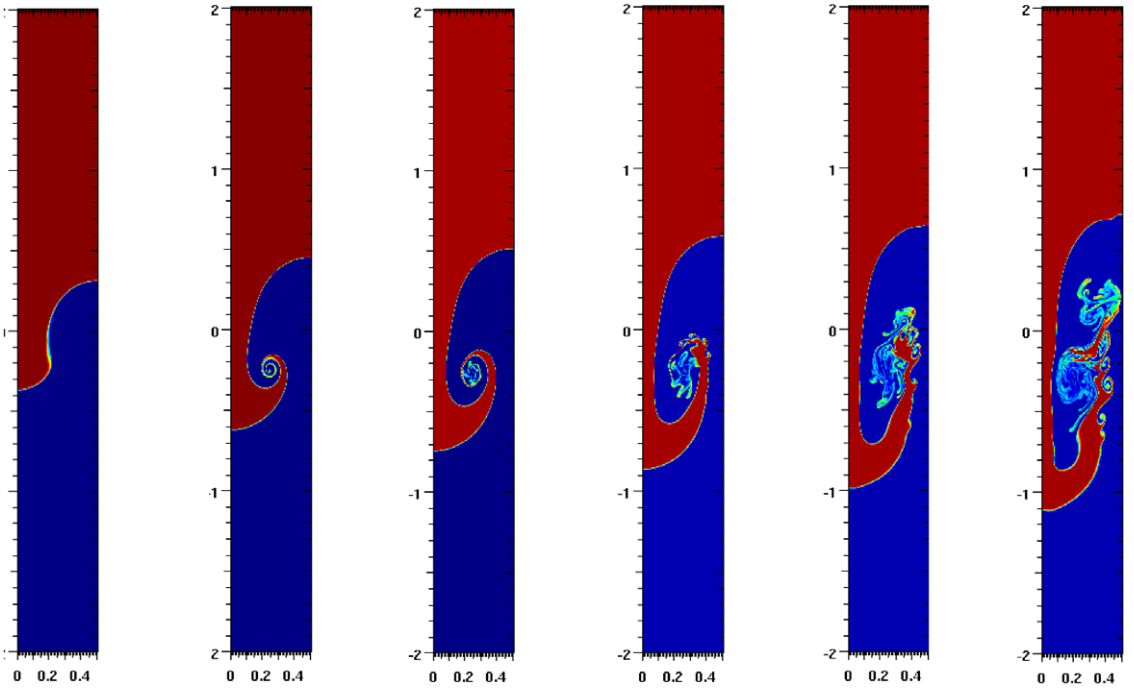

Fig. 2. $Re = 5000$; density ratio 3. The interface is shown at times 1, 1.5, 1.75, 2, 2.25, and 2.5.

Please cite this article in press as: J.-L. Guermond, A. Salgado, A splitting method for incompressible flows with variable density ..., J. Comput. Phys. (2009), doi:10.1016/j.jcp.2008.12.036

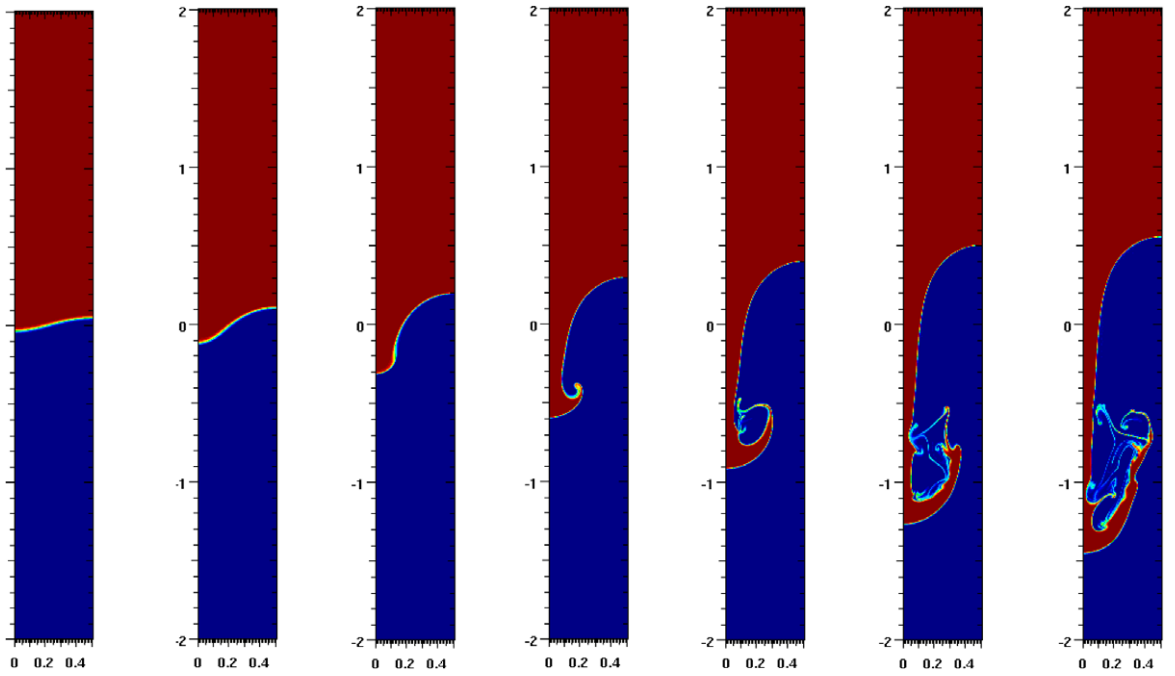

Fig. 3. $Re = 1000$; density ratio 7. The interface is shown at times 1, 1.5, 2, 2.5, 3, 3.5, and 3.75.

To further assess the sensitivity of the method to spatial resolution and to verify that the numerical viscosity is significantly smaller than the physical viscosity we solve the same problem using the same mesh for $Re = 5000$. The results are shown in Fig. 2.

The above results are in good agreement with those from [8]. Since the algorithm (4.1)–(4.4), only requires solving a Poisson equation, computing the above test cases was significantly faster (one order of magnitude) than when doing the computations reported in [8]. This time saving allowed us to use finer space resolution.

5.3. High Atwood number

We finish by performing a test case reported in [2]. The geometry is the same as in Section 5.2. The density ratio is 7 so that $A_t = 0.75$, using Tryggvason's definition (5.2) (using the definition from [2] the Atwood number is 0.875). The initial density field is regularized as follows:

$$\frac{\rho(x,y,t=0)}{\rho_0^{\min}} = 4 + 3\tanh\left(\frac{y-\eta(x)}{0.01d}\right), \tag{5.3}$$

where the perturbation of the interface is given by $\eta(x) = -0.01d\cos(2\pi x/d)$. The Reynolds number is $Re = 1000$.

The results using the same mesh and same time step as in Section 5.2 are reported in Fig. 3 for times 1, 1.5, 2, 2.5, 3, 3.5, and 3.75 (using $d^{1/2}/g^{1/2}$ as time scale). Although the locations of the falling and rising bubbles are similar to those reported in [2], the details of the flow differ from those in [2]. This unexplained discrepancy was already noted in [18].

Acknowledgments

The authors are supported by the National Science Foundation Grants DMS-0510650 and DMS-0713829.

References

[1] Ann S. Almgren, John B. Bell, Phillip Colella, Louis H. Howell, Michael L. Welcome, A conservative adaptive projection method for the variable density incompressible Navier–Stokes equations, J. Comput. Phys. 142 (1) (1998) 1–46.
[2] John B. Bell, Daniel L. Marcus, A second-order projection method for variable-density flows, J. Comput. Phys. 101 (1992) 334–348.
[3] F. Brezzi, M. Fortin, Mixed and Hybrid Finite Element Methods, Springer-Verlag, New York, NY, 1991.
[4] D.L. Brown, R. Cortez, M.L. Minion, Accurate projection methods for the incompressible Navier–Stokes equations, J. Comput. Phys. 168 (2) (2001) 464–499.
[5] A.J. Chorin, Numerical solution of the Navier–Stokes equations, Math. Comput. 22 (1968) 745–762.
[6] J. Douglas Jr., T.F. Russell, Numerical methods for convection-dominated diffusion problems based on combining the method of characteristics with finite element or finite difference procedures, SIAM J. Numer. Anal. 19 (1982) 871–885.

[7] A. Ern, J.-L. Guermond, Theory and Practice of Finite Elements, Applied Mathematical Sciences, vol. 159, Springer-Verlag, New York, 2004.
[8] Y. Fraigneau, J.-L. Guermond, L. Quartapelle, Approximation of variable density incompressible flows by means of finite elements and finite volumes, Commun. Numer. Methods Eng. 17 (2001) 893–902.
[9] V. Girault, P.-A. Raviart, Finite Element Methods for Navier–Stokes Equations Theory and Algorithms Springer Series in Computational Mathematics, Springer-Verlag, Berlin, Germany, 1986.
[10] J.-L. Guermond, Some practical implementations of projection methods for Navier–Stokes equations, M2AN Math. Model. Numer. Anal. 30 (5) (1996) 637–667.
[11] J.-L. Guermond, Un résultat de convergence d'ordre deux en temps pour l'approximation des équations de Navier–Stokes par une technique de projection incrémentale, M2AN Math. Model. Numer. Anal. 33 (1) (1999) 169–189. Also in C.R. Acad. Sci. Paris, Série I, 325:1329–1332, 1997.
[12] J.-L. Guermond, A. Marra, L. Quartapelle, Subgrid stabilized projection method for 2d unsteady flows at high Reynolds number, Comput. Methods Appl. Mech. Eng. 195 (2006).
[13] J.L. Guermond, P. Minev, Jie Shen, An overview of projection methods for incompressible flows, Comput. Methods Appl. Mech. Eng. 195 (44–47) (2006) 6011–6045.
[14] J.-L. Guermond, R. Pasquetti, Entropy-based nonlinear viscosity for fourier approximations of conservation laws, C.R. Math. Acad. Sci. Paris, 346 (2008) 913–918.
[15] J.-L. Guermond, R. Pasquetti, B. Popov, Entropy-based viscosities, in preparation.
[16] J.-L. Guermond, L. Quartapelle, Calculation of incompressible viscous flows by an unconditionally stable projection FEM, J. Comput. Phys. 132 (1) (1997) 12–33.
[17] J.-L. Guermond, L. Quartapelle, On the approximation of the unsteady Navier–Stokes equations by finite element projection methods, Numer. Math. 80 (5) (1998) 207–238.
[18] J.-L. Guermond, L. Quartapelle, A projection FEM for variable density incompressible flows, J. Comput. Phys. 165 (1) (2000) 167–188.
[19] J.-L. Guermond, J. Shen, On the error estimates for the rotational pressure-correction projection methods, Math. Comput. 73 (248) (2004) 1719–1737. electronic.
[20] T.J.R. Hughes, L.P. Franca, G.M. Hulbert, A new finite element formulation for computational fluid dynamics: VIII. The Galerkin/Least-Squares method for advection-diffusive equations, Comput. Methods Appl. Mech. Eng. 73 (1989) 173–189.
[21] C. Johnson, U. Nävert, J. Pitkäranta, Finite element methods for linear hyperbolic equations, Comput. Methods Appl. Mech. Eng. 45 (1984) 285–312.
[22] P.-L. Lions, Mathematical topics in fluid mechanics, vol. 1. Incompressible models, Oxford Lecture Series in Mathematics and its Applications, vol. 3. The Clarendon Press, Oxford University Press, New York, 1996.
[23] Chun Liu, Noel J. Walkington, Convergence of numerical approximations of the incompressible Navier–Stokes equations with variable density and viscosity, SIAM J. Numer. Anal. 45 (3) (2007) 1287–1304. electronic.
[24] Jae-Hong Pyo, Jie Shen, Gauge-Uzawa methods for incompressible flows with variable density, J. Comput. Phys. 221 (1) (2007) 181–197.
[25] R. Rannacher, On Chorin's projection method for the incompressible Navier–Stokes equations, in: The Navier–Stokes Equations II—Theory and Numerical Methods (Oberwolfach, 1991), Lecture Notes in Math., vol. 1530, Springer, Berlin, Germany, 1992, pp. 167–183.
[26] J. Shen, On error estimates of projection methods for the Navier–Stokes equations: first-order schemes, SIAM J. Numer. Anal. 29 (1992) 57–77.
[27] J. Shen, Efficient Chebyshev–Legendre Galerkin methods for elliptic problems, in: A.V. Ilin, R.L. Scott (Eds.), Proceedings of ICOSAHOM'95, Houston J. Math., 1996, pp. 233–240.
[28] R. Temam, Sur l'approximation de la solution des équations de Navier–Stokes par la méthode des pas fractionnaires II, Arch. Rat. Mech. Anal. 33 (1969) 377–385.
[29] Roger Temam, Une méthode d'approximation de la solution des équations de Navier–Stokes, Bull. Soc. Math. France 96 (1968) 115–152.
[30] L.J.P. Timmermans, P.D. Minev, F.N. van de Vosse, An approximate projection scheme for incompressible flow using spectral elements, Int. J. Numer. Methods Fluids 22 (1996) 673–688.
[31] G. Tryggvason, Numerical simulation of Rayleigh–Taylor instability, J. Comput. Phys. 75 (1988) 253–282.
[32] N.J. Walkington, Convergence of the discontinuous Galerkin method for discontinuous solutions, SIAM J. Numer. Anal. 42 (5) (2004) 1801–1817.

Please cite this article in press as: J.-L. Guermond, A. Salgado, A splitting method for incompressible flows with variable density ..., J. Comput. Phys. (2009), doi:10.1016/j.jcp.2008.12.036